The synthesis and properties of $Pt_2 \rightarrow M$ (M = Ag(I), Hg(II)) adducts of $Pt_2\{o\text{-}C_6H_4P(Ph)(CH_2)_3PPh_2\}_2$ with $Ag(O_2CCF_3)$, $HgCl_2$ and $Hg(O_2CCF_3)_2$. X-ray crystal structure of $[Pt_2\{o\text{-}C_6H_4P(Ph)(CH_2)_3PPh_2\}_2Hg(O_2CCF_3)_2]$

G. P. C. M. Dekker, C. J. Elsevier, S. N. Poelsma, K. Vrieze*

Anorganisch Chemisch Laboratorium, J. H. van't Hoff Instituut, Universiteit van Amsterdam, Nieuwe Achtergracht 166, 1018 WV Amsterdam (Netherlands)

P. W. N. M. van Leeuwen

Department of Chemical Engineering, J. H. van't Hoff Instituut, University of Amsterdam, Nieuwe Achtergracht 166, 1018 WV Amsterdam (Netherlands)

W. J. J. Smeets and A. L. Spek

Bijvoet Center for Biomolecular Research, vakgroep Kristal- en Structuurchemie, University of Utrecht, Padualaan 8, 3584 CH Utrecht (Netherlands)

(Received October 3, 1991; revised February 7, 1992)

Abstract

During the attempted synthesis of (dppp)Pt(C_2H_4) (dppp = 1,3-bis(diphenylphosphino)propane) a Pt(I)–Pt(I) dimer, $Pt_2\{o\text{-}C_6H_4P(Ph)(CH_2)_3PPh_2\}_2$, was formed in approximately 5–10% yield. In this dimer the dppp ligand coordinates with two phosphorus atoms to one Pt centre, while one of the phenyl groups of the ligand is *ortho*-metallated to the second Pt centre. The reaction of this Pt(I)–Pt(I) dimer with $Ag(O_2CCF_3)$, $HgCl_2$ and $Hg(O_2CCF_3)_2$ resulted in the formation of Pt_2-to-M donor adducts $[Pt_2\{o\text{-}C_6H_4P(Ph)(CH_2)_3PPh_2\}_2Z]$ (Z = $Ag(O_2CCF_3)$, $HgCl_2$ and $Hg(O_2CCF_3)_2$) in which the Pt–Pt bond, although weakened, remained intact. The $^{31}P\{^1H\}$ NMR spectra showed, with increasing electronegativity of Z, an increase in coupling constant ^1J(Pt–P1) and a decrease in coupling constant ^1J(Pt'–P1) for the approximately linear P1–Pt–Pt'–P1' unit, indicating a weaker Pt–Pt bond and a stronger $Pt_2 \rightarrow M$ bond in the order M = Hg(II) > Ag(I). An X-ray structure of the red-brown crystals of $[Pt_2\{o\text{-}C_6H_4P(Ph)(CH_2)_3PPh_2\}_2Hg(O_2CCF_3)_2]$ has been determined (space group *Cc2a*, $a = 14.392(2)$, $b = 19.950(1)$, $c = 19.427(1)$ Å, $V = 5577.9(9)$ Å^3, $Z = 4$, $R = 0.038$, $R_w = 0.061$). The structure shows a Pt–Hg–Pt triangle with bond lengths Pt–Pt = 2.7608(7) and Pt–Hg = 2.6690(10) Å.

Introduction

Orthometallation of P donor ligands at the metal at which the P donor atom coordinates has been described for several metals [1]. Mass spectrometric studies of $(PPh_3)_2Pt(Ph)_2$ [2] and *trans*-$(PPh_3)_2Pt(H)Cl$ [3] showed that, on heating, *ortho*-metallated complexes were formed together with volatile products such as H_2 and benzene. Orthometallation of P donor ligands at bimetallic centres has also been reported for several metal complexes [4–8]. The reactivity of *ortho*-metallated complexes towards reagents such as CH_3I was described for $Pt_2\{o\text{-}C_6H_4P(Ph)(CH_2)_2PPh_2\}_2$ by Arnold *et al.* [9, 10]. This reaction yielded an oxidized Pt(II)–Pt(II) complex, $[Pt_2\{o\text{-}C_6H_4P(Ph)(CH_2)_2PPh_2\}_2CH_3]^+I^-$, in which the metal–metal bond was broken [9]. Recently the reactivity of some *ortho*-metallated Pt(I)–Pt(I) dimers, $(Pt_2\{o\text{-}C_6H_4P(Ph)(CH_2)_nPPh_2\}_2$ ($n = 2$, 3) and $Pt_2\{o\text{-}C_6H_4PPh_2\}_2(PPh_3)_2$) towards $Au(PPh_3)BF_4$ has been described [11]. In these reactions the Pt–Pt bond remained intact, although changes were observed in the $^{31}P\{^1H\}$ NMR spectra. An X-ray crystal structure analysis of $[Pt_2\{o\text{-}C_6H_4P(Ph)(CH_2)_3PPh_2\}_2Au(PPh_3)]^+BF_4^-$ (Scheme 1) revealed that the $Au(PPh_3)$ unit is bridging between the two Pt atoms [11], with a Pt–Pt distance of 2.703 Å and Pt–Au distances of 2.722(1) and 2.697(1) Å. From NMR and X-ray data it was concluded that the Pt–Pt bond in the Au(I) adduct was weakened relative to that in the starting compound.

In this article we report the formation of the dimer $Pt_2\{o\text{-}C_6H_4P(Ph)(CH_2)_3PPh_2\}_2$ (**1**) (Scheme 1), which

*Author to whom correspondence should be addressed.

0020-1693/92/$5.00

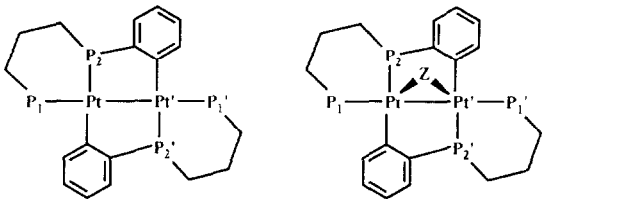

$Pt_2\{o\text{-}C_6H_4P(Ph)(CH_2)_3PPh_2\}_2$ (1) Z=$Ag(O_2CCF_3)$ (2)
Z=$HgCl_2$ (3)
Z=$Hg(O_2CCF_3)_2$ (4)
Z=$Au(PPh_3)^+$ (5) (BF_4^- as counteranion) [11]
Z=I^+ (6) (I^- as counteranion) [11]

Scheme 1. Schematic structure of $Pt_2\{o\text{-}C_6H_4P(Ph)(CH_2)_3PPh_2\}_2$ (**1**) and the products of its reaction with $Ag(O_2CCF_3)$, $HgCl_2$ and $Hg(O_2CCF_3)_2$ (this work), $Au(PPh_3)^+BF_4^-$ [11] and I_2 [11].

was formed during the attempted synthesis of (dppp)Pt(C_2H_4) according to the method described by Nagel for (dppe)Pt(C_2H_4) [12]. The products of **1** with $Ag(O_2CCF_3)$, $HgCl_2$ and $Hg(O_2CCF_3)_2$, i.e. $[Pt_2\{o\text{-}C_6H_4P(Ph)(CH_2)_3PPh_2\}_2Ag(O_2CCF_3)]$ (**2**), $[Pt_2\{o\text{-}C_6H_4P(Ph)(CH_2)_3PPh_2\}_2HgCl_2]$ (**3**) and $[Pt_2\{o\text{-}C_6H_4P(Ph)(CH_2)_3PPh_2\}_2Hg(O_2CCF_3)_2]$ (**4**), respectively (Scheme 1), have been studied by means of $^{31}P\{^1H\}$ NMR spectroscopy and appear to be similar to the complex $[Pt_2\{o\text{-}C_6H_4P(Ph)(CH_2)_3PPh_2\}_2Au(PPh_3)]^+BF_4^-$ [11], which was reported in the course of the preparation of this manuscript. The X-ray crystal structure of the product formed in the reaction of **1** with $Hg(O_2CCF_3)_2$, i.e. $[Pt_2\{o\text{-}C_6H_4P(Ph)(CH_2)_3PPh_2\}_2Hg(O_2CCF_3)_2]$ (**4**), will be described.

Experimental

All reactions and manipulations were carried out under purified nitrogen using Schlenk techniques. ^1H and $^{31}P\{^1H\}$ NMR spectra were recorded on a Bruker AC 100 spectrometer at 100.13 and 40.53 MHz, respectively. Shifts are relative to $(CH_3)_4Si$ (^1H) and 85% H_3PO_4 (^{31}P) as external standards, where positive shifts are to high frequency. Simulations of the spectra were carried out at the Koninklijke/Shell-Laboratorium Amsterdam with the program geNMR, version 3.1 (IvorySoft, Amsterdam, 1989). CH_2Cl_2 was dried over P_2O_5. Ethanol (p.a.) was used without purification. (COD)$PtCl_2$ (COD = 1,5-cyclooctadiene) was prepared according to published methods [13]. Ethene was obtained from Matheson. $Ag(O_2CCF_3)$, $HgCl_2$ and $Hg(O_2CCF_3)_2$ were obtained from Merck and used without purification.

$[Pt_2\{o\text{-}C_6H_4P(Ph)(CH_2)_3PPh_2\}_2]$ (1)

A gentle stream of ethene (*c.* 100 ml/min) was passed through a slurry of (dppp)$PtCl_2$ (3.30 g, 4.9 mmol) in a 1:1 mixture of CH_2Cl_2/ethanol (50 ml) for 15 min, while cooling to 10 °C. Then, 5 equiv. of $NaBH_4$ (0.95 g, 25 mmol) were added in small portions over a period of 30 min, while maintaining an ethene atmosphere by very slowly bubbling ethene through the solution. Gradually the slurry became yellow. After this addition ethene was bubbled through for another 15 min and then ethanol (100 ml) was added. After filtration the yellow–orange solution was allowed to stand overnight, during which period the colour became darker and eventually a brown solution was obtained. After 12 h yellow crystals separated in a yield of 0.29 g (5%), together with unidentified products. *Anal.* Calc. for $C_{54}H_{50}P_4Pt_2 \cdot CH_2Cl_2$ (**1**): C, 50.89; H, 4.04; P, 9.55. Found: C, 51.14; H, 4.24; P, 9.32%.

$[Pt_2\{o\text{-}C_6H_4P(Ph)(CH_2)_3PPh_2\}_2Ag(O_2CCF_3)]$ (2)

To a solution of **1** (0.18 g, 0.15 mmol) in 15 ml CH_2Cl_2 1 equiv. of $Ag(O_2CCF_3)$ (0.033 g, 0.15 mmol) was added. The solution changed gradually in colour from yellow to green and then to brown. The mixture was stirred for 1 h after which diethyl ether was added. The product precipitated and was washed with diethyl ether (2×3 ml). The yield was 0.12 g (57%) of green-brown powder. *Anal.* Calc. for $C_{56}H_{50}O_2F_3P_4Pt_2Ag$ (**2**): C, 46.90; H, 3.52; P, 8.63. Found: C, 46.83; H, 3.65; P: 8.71%.

$[Pt_2\{o\text{-}C_6H_4P(Ph)(CH_2)_3PPh_2\}_2HgCl_2]$ (3) and $[Pt_2\{o\text{-}C_6H_4P(Ph)(CH_2)_3PPh_2\}_2Hg(O_2CCF_3)_2]$ (4)

The synthesis of these compounds was carried out in a way analogous to the synthesis of **2**, adding 0.041 g (0.15 mmol) $HgCl_2$ or 0.064 g (0.15 mmol) $Hg(O_2CCF_3)_2$, respectively. Both **3** and **4** had 1 molecule of CH_2Cl_2 encapsulated. Yield; 69% of pale brown powder (**3**); 63% of red–brown powder (**4**). *Anal.* Calc. for $C_{54}H_{50}P_4Cl_2Pt_2Hg \cdot CH_2Cl_2$ (**3**): C, 41.34; H, 3.34; P, 7.89. Found: C, 41.41; H, 3.41; P, 7.70%. Calc. for $C_{58}H_{50}O_4F_6P_4Pt_2Hg \cdot CH_2Cl_2$ (**4**): C, 41.09; H, 3.04; P, 6.77. Found: C, 40.33; H, 3.14; P, 7.18%.

Structure determination and refinement of $[Pt_2\{o\text{-}C_6H_4P(Ph)(CH_2)_3PPh_2\}_2Hg(O_2CCF_3)_2]$ (4)

A red–brown block shaped crystal was mounted on top of a glass fiber and transferred to an Enraf-Nonius CAD4 diffractometer for data collection (100 K). Unit cell parameters were determined from a least-squares treatment of the setting angles [14] of 25 reflections with $12.3 < \theta < 19.4°$. The unit cell parameters were checked for the presence of higher lattice symmetry [15]. The quality of the crystal was rather poor; the crystal appeared to consist of two parts rotated by 2.7°, intensity data were collected for one of the lattices. Data were corrected for Lorentz–polarization, for a linear decay (2.0%) of the intensity control reflections

during the 63 h of X-ray exposure time and absorption (DIFABS absorption correction was applied after the atoms were located [16]). The structure was solved with standard Patterson methods (revealing the Pt and Hg positions) (SHELXS86 [17]) and subsequent difference Fourier analyses. Refinement on F was carried out by full matrix least-squares techniques. H atoms were introduced on calculated positions (C–H = 0.98 Å) and included in the refinement riding on their carrier atoms. In view of the limited quality of the data, only the non-C, H atoms were refined with anisotropic thermal parameters. The C atoms were refined isotropically; H atoms with one common isotropic thermal parameter ($U = 0.012(9)$ Å^2). Weights were introduced in the final refinement cycles, convergence was reached at $R = 0.038$. A few reflections were left out of the refinement cycles in view of overlapping data. The absolute structure was checked by refinement with opposite f'' anomalous dispersion factors, resulting in $R = 0.046$, $R_w = 0.071$.

Crystal data and numerical details of the structure determination are given in Table 1. Final atomic coordinates and equivalent isotropic thermal parameters are listed in Table 2. Neutral atom scattering factors were taken from ref. 18 and corrected for anomalous dispersion [19]. All calculations were performed with SHELX76 [20] and the EUCLID package [21] (geometrical calculations and illustrations) on a MicroVAX cluster.

TABLE 1. Crystal data and details of the structure determination of $[Pt_2\{o\text{-}C_6H_4P(Ph)(CH_2)_3PPh_2\}_2Hg(O_2CCF_3)_2]$ (**4**)

Crystal data	
Formula	$C_{58}H_{50}F_6O_4P_4HgPt_2 \cdot CH_2Cl_2$
Molecular weight	1724.59
Crystal system	orthorhombic
Space group	*Cc2a* (*bca* setting of *Aba*2; No. 41[a])
a, b, c (Å)	14.392(2), 19.950(1), 19.427(1)
V (Å^3)	5577.9(9)
Z	4
D_{calc} (g cm^{-3})	2.0535(3)
$F(000)$	3288
μ (cm^{-1})	80.8
Crystal size (mm)	0.30×0.32×0.35
Data collection	
Temperature (K)	100
θ_{min}, θ_{max}	1.05, 27.50
Radiation	Mo Kα (Zr-filtered), 0.71073 Å
Scan type	$\omega/2\theta$
$\Delta\omega$ (°)	0.60 + 0.35 tanθ
Horizontal and vertical aperture (mm)	3.0, 5.0
Distance from crystal to detector (mm)	173
Reference reflections	0−22, −202, −440
Data set	h −18:0; k −25:0; l 0:25
Total data	3624
Total unique data	3285
Observed data	2874 ($I > 2.5\sigma(I)$)
DIFABS correction range	0.875 − 1.195
Refinement	
No. of refined parameters	204
Weighting scheme	$w = 1.0/[\sigma^2(F) + 0.005554F^2]$
Final R, R_w	0.038, 0.061
$(\Delta/\sigma)_{av}$, $(\Delta/\sigma)_{max}$ in final cycle	0.048, 0.343
Min. and max. residual density (e/Å^3)	−1.79, 1.53 (near Pt, Hg)

[a]Equivalent positions: $-x, y, -z$; $\frac{1}{2}+x, y, \frac{1}{2}-z$; $\frac{1}{2}-x, y, \frac{1}{2}+z$.

TABLE 2. Final coordinates and equivalent isotropic thermal parameters of the non-hydrogen atoms for **4**

Atom	x	y	z	U_{eq} (Å^2)[a]
Hg	0	0	0	0.0087(2)
Pt	0.06584(3)	0.11450(5)	0.05167(2)	0.0056(1)
P(1)	0.1621(2)	0.14535(19)	0.13991(17)	0.0070(9)
P(2)	−0.0681(2)	0.14872(19)	0.10722(19)	0.0084(9)
F(1)	−0.0126(7)	−0.1195(5)	0.2444(5)	0.028(3)
F(2)	0.0574(9)	−0.1777(6)	0.1700(6)	0.035(4)
F(3)	0.1278(8)	−0.0993(7)	0.2191(6)	0.044(4)
O(1)	−0.0150(10)	−0.0108(8)	0.1570(6)	0.040(4)
O(2)	0.0311(10)	−0.0839(7)	0.0751(6)	0.023(3)
C(1)	0.1673(8)	0.0987(6)	−0.0820(6)	0.005(2)
C(2)	0.2354(9)	0.0778(7)	−0.1292(7)	0.010(3)
C(3)	0.3026(11)	0.0344(8)	−0.1096(8)	0.018(3)
C(4)	0.3065(12)	0.0101(8)	−0.0432(8)	0.017(3)
C(5)	0.2391(10)	0.0319(7)	0.0049(7)	0.011(3)
C(6)	0.1703(10)	0.0785(7)	−0.0113(7)	0.011(3)
C(7)	0.0174(10)	−0.0648(8)	0.1358(8)	0.014(3)
C(8)	0.0465(11)	−0.1160(9)	0.1931(8)	0.019(3)
C(9)	−0.0681(9)	0.1452(7)	0.2017(7)	0.008(3)
C(10)	0.0184(10)	0.1791(8)	0.2333(8)	0.015(3)
C(11)	0.1058(9)	0.1345(7)	0.2241(7)	0.011(3)
C(12)	−0.1000(9)	0.2365(7)	0.0949(6)	0.007(2)
C(13)	−0.0355(13)	0.2830(9)	0.0809(9)	0.020(3)
C(14)	−0.0604(12)	0.3511(11)	0.0797(10)	0.026(4)
C(15)	−0.1515(12)	0.3709(9)	0.0868(9)	0.023(4)
C(16)	−0.2179(13)	0.3232(9)	0.0995(9)	0.028(4)
C(17)	−0.1928(11)	0.2544(8)	0.1047(8)	0.018(3)
C(18)	0.2684(10)	0.0968(7)	0.1526(7)	0.014(3)
C(19)	0.2656(10)	0.0370(7)	0.1907(7)	0.012(3)
C(20)	0.3486(9)	0.0008(8)	0.1983(7)	0.012(3)
C(21)	0.4297(9)	0.0199(7)	0.1663(7)	0.009(3)
C(22)	0.4298(12)	0.0775(9)	0.1255(9)	0.023(3)
C(23)	0.3502(10)	0.1155(11)	0.1198(7)	0.020(3)
C(24)	0.2081(10)	0.2304(8)	0.1408(7)	0.015(3)
C(25)	0.2375(11)	0.2597(9)	0.2016(8)	0.020(3)
C(26)	0.2816(12)	0.3228(9)	0.1992(9)	0.023(3)
C(27)	0.2902(13)	0.3567(10)	0.1376(9)	0.028(4)
C(28)	0.2621(12)	0.3269(8)	0.0775(8)	0.019(3)
C(29)	0.2213(11)	0.2647(8)	0.0801(8)	0.014(3)
Dichloromethane solvate				
Cl	0.5836(4)	0.2144(3)	0.0420(3)	0.0327(14)
C(30)	1/2	0.2653(17)	0	0.037(7)

[a]U_{eq} = 1/3 of the trace of the orthogonalized U matrix.

Results and discussion

Synthesis of $Pt_2\{o\text{-}C_6H_4P(Ph)(CH_2)_3PPh_2\}_2$ (1) and of the adducts with $Ag(O_2CCF_3)$, $HgCl_2$ and $Hg(O_2CCF_3)_2$

During the attempted preparation of (dppp)Pt(C_2H_4) by reduction of (dppp)$PtCl_2$ with $NaBH_4$ under C_2H_4 atmosphere in CH_2Cl_2/ethanol, in addition to unidentified products, a fine yellow powder was collected in a yield of 5–10% after leaving the solution for 24 h. Analysis by $^{31}P\{^1H\}$ NMR revealed that the yellow compound is the bis-*ortho*-metallated Pt(I)–Pt(I) dimer, $Pt_2\{o\text{-}C_6H_4P(Ph)(CH_2)_3PPh_2\}_2$ (**1**) (Scheme 1), which was recently reported to be formed upon heating of (dppp)Pt(CH_3)Cl with sodium methoxide in methanol [11]. Attempts to grow suitable crystals of **1** for a satisfactory X-ray crystal structure analysis failed*.

Reaction of **1** with $Ag(O_2CCF_3)$, $HgCl_2$ and $Hg(O_2CCF_3)_2$ resulted in the formation of complexes $[Pt_2\{o\text{-}C_6H_4P(Ph)(CH_2)_3PPh_2\}_2Ag(O_2CCF_3)]$ (**2**), $[Pt_2\{o\text{-}C_6H_4P(Ph)(CH_2)_3PPh_2\}_2HgCl_2]$ (**3**) and $[Pt_2\{o\text{-}C_6H_4P(Ph)(CH_2)_3PPh_2\}_2Hg(O_2CCF_3)_2]$ (**4**), which appear to be similar to $[Pt_2\{o\text{-}C_6H_4P(Ph)(CH_2)_3PPh_2\}_2Au(PPh_3)]^+BF_4^-$ [11] (Scheme 1).

X-ray structure of $[Pt_2\{o\text{-}C_6H_4P(Ph)(CH_2)_3PPh_2\}_2Hg(O_2CCF_3)_2]$ (4)

The molecular structure of $[Pt_2\{o\text{-}C_6H_4P(Ph)(CH_2)_3PPh_2\}_2Hg(O_2CCF_3)_2]$ (**4**) consists of a triangle formed by the Hg atom and the two Pt atoms (Fig. 1). The molecule has a two-fold symmetry axis through Hg perpendicular to the Pt–Pt bond. The phosphorus atoms lie below the mean plane of the $Pt_2P_4(C_{ortho})_2$ unit of **1** due to the complexation of Hg above this plane in **4**. Four non-*ortho*-metallated phenyl groups also lie below this plane and point away from the Hg atom. The other two phenyl groups as well as the *ortho*-metallated phenyl groups are pointing upwards and lie above the plane.

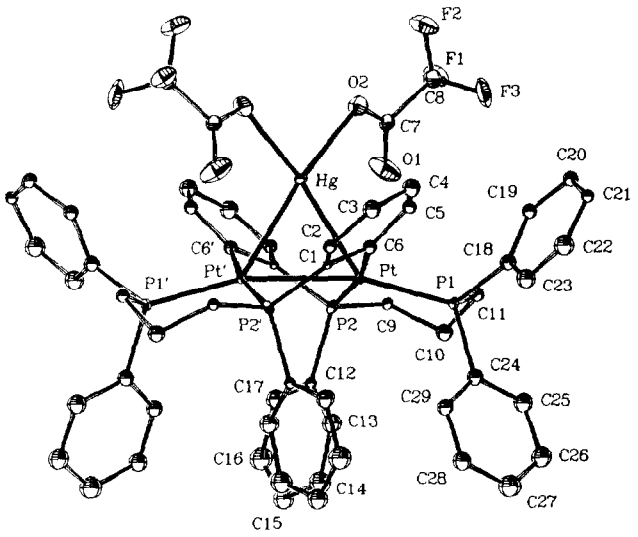

Fig. 1. Thermal motion ellipsoid plot drawn at 50% probability level (H atoms omitted) for the molecular structure of $[Pt_2\{o\text{-}C_6H_4P(Ph)(CH_2)_3PPh_2\}_2Hg(O_2CCF_3)_2]$ (**4**).

TABLE 3. Selected bond distances (Å) and angles (°) of $[Pt_2\{o\text{-}C_6H_4P(Ph)(CH_2)_3PPh_2\}_2Hg(O_2CCF_3)_2]$ (**4**)[a]

Pt–Pt'	2.7608(7)	Pt–Hg–Pt'	62.29(2)
Pt–Hg	2.6690(10)	Hg–Pt–P1	136.62(10)
Pt–P1	2.288(3)	Hg–Pt–P2	97.60(9)
Pt–P2	2.312(3)	Hg–Pt–C6	74.8(4)
Pt–C6	2.067(14)	Hg–Pt–Pt'	58.86(2)
		P1–Pt–P2	94.34(12)
		P1–Pt–C6	95.5(4)
		Pt'–Pt–P1	163.80(10)
		P2–Pt–C6	170.1(4)
		Pt'–Pt–P2	76.53(9)
		Pt'–Pt–C6	94.0(4)

[a]Prime indicates symmetry operation $-x, y, -z$.

The Pt–P2 distances of 2.312(3) Å in **4** (Table 3) do not differ significantly from the distances found in **5** [11] for Pt–P2 (2.303(6) Å) and Pt'–P2' (2.306(7) Å) showing that the P–Pt bonds perpendicular to the Pt–Pt bond do not change much upon changes in the Pt–Pt bond. The two Pt–C6 distances amount to 2.067(14) Å in **4** and 2.07(3) and 2.05(3) Å in **5**, which also illustrates the insensitivity of the metal–ligand bonds perpendicular to the Pt–Pt bond with respect to adduct formation. This is also reflected in the minor changes in the coupling constants ^1J(Pt–P2) and ^2J(Pt'–P2) (see below, Table 4). A significant difference in the bond lengths of Pt–P1 and Pt'–P1' is observed when **4** and **5** are compared: 2.288(3) Å in **4** and 2.305(6) and

*X-ray structure of $[Pt_2\{o\text{-}C_6H_4P(Ph)(CH_2)_3PPh_2\}_2]$ (**1**), (K. F. van Malssen, University of Amsterdam). Crystals of compound $[Pt_2\{o\text{-}C_6H_4P(Ph)(CH_2)_3PPh_2\}_2]$ are monoclinic, space group $P2_1/n$, $a = 11.192(1)$, $b = 20.866(5)$, $c = 21.363(4)$ Å; $\beta = 103.68(2)°$; $Z = 4$. Data collection was performed on an Enraf-Nonius CAD4 diffractometer using graphite-monochromated Cu Kα radiation (λ(Cu Kα) = 1.5418 Å) at room temperature for reflections with $2.5 \leq \theta \leq 40°$ (this upper limit is low due to poor quality of the crystals). The limited number of data (1246 observed reflections) permitted only anisotropic refinement for the Pt and P atoms, the C atoms were refined isotropically and no attempt was made to determine the H atoms. An empirical absorption correction was applied, DIFABS 0.45–1.44. Final $R = 0.071$. Maximum $\Delta/\sigma = 0.84$. Therefore, only the following distances are reliable: Pt–Pt' = 2.656(5), Pt–P1 = 2.25(3), Pt'–P1' = 2.279(20), Pt–P2 = 2.27(3), Pt'–P2' = 2.251(19), Pt–C6 = 2.10(9), Pt'–C6' = 2.05(7) Å. The Pt–P2 and Pt'–P2' distances as well as the Pt–P1 and Pt'–P1' distances do not differ significantly from the distances found for $Pt_2\{o\text{-}C_6H_4P(Ph)(CH_2)_2PPh_2\}_2$: av. Pt–P2 = 2.240, av. Pt–P1 = 2.272 Å [5]. The Pt–Pt bond is significantly longer: 2.656(5) Å in **1** and 2.628(1) Å in $Pt_2\{o\text{-}C_6H_4P(Ph)(CH_2)_2PPh_2\}_2$ [5]. In $[Pt_2(dppp)_2(2,4,6\text{-}(CH_3)_3C_6H_2NC)_2](PF_6)_2$, where no *ortho*-metallation has taken place, the Pt–Pt bond distance of 2.653(2) Å [22] does not differ significantly from **1** (2.656(5) Å).

2.320(6) Å in **5**. The elongation of the Pt–Pt bond in **4** (2.7608(7) Å) relative to **5** (2.703(1) Å) is an indication of a weaker Pt–Pt bond in **4** as compared to **5**. The Hg–Pt distance of 2.6690(10) Å is significantly shorter than the Hg–Pt distances of 2.7122(8) and 2.7153(7) Å and of 2.6991(8) and 2.7097(8) Å found in two crystal forms of $Pt_2(\mu\text{-}HgCl_2)Cl_2(dppm)_2$ [23], in which $HgCl_2$ is bridging the Pt–Pt bond.

Correlation of the ^{31}P NMR data of complexes 1–6 with the $Pt_2 \rightarrow M$ (M = Hg(II), Au(I) and Ag(I)) bond strength

The ^{31}P NMR spectra show that the various Group 11 and 12 metal atoms differ in their interaction with the metal–metal bond, as is reflected by the differences in the spin–spin coupling constants (Table 4). The coupling ^1J(Pt–P2) decreases slightly when going from **1** (Pt–Pt bond present, ^1J(Pt–P2) = 1860 Hz) to **6** (no Pt–Pt bond present, ^1J(Pt–P2) = 1664 Hz), which shows that a change in the metal–metal bond has little influence on the Pt–P2 and Pt′–P2′ bonds, i.e. the Pt–P bonds perpendicular to the Pt–Pt bond. When the metal–metal bond is broken the coupling ^2J(Pt′–P2), however, which is probably transmitted via the metal–metal bond, decreases; in **1** the coupling constant amounts to −143 Hz while in **6** no coupling ^2J(Pt′–P2) was observed [11]. The coupling between Pt′ and P1 is still present after breaking of the bond (**6**) although it is very small: 996 Hz in **1** and 73 Hz in **6**. The presence of the coupling between Pt′ and P1 in **6** implies that the coupling is probably transmitted via the bridging iodide atom, meaning that the coupling ^2J(Pt′–P1) in **1** is best described in **6** as ^3J(Pt′–P1); it seems unlikely that the coupling is transmitted via the organic backbone, which would require a ^5J(Pt′–P1) coupling in **6**. The coupling ^1J(Pt–P1) increases strongly upon breaking of the Pt–Pt bond, indicating that P1 has a much stronger σ-interaction with Pt in **6** (^1J(Pt–P1) = 3719 Hz) than in **1** (^1J(Pt–P1) = 1775 Hz). The small value in **1** shows that the Pt–Pt bond has a *trans* influence which is comparable to that of an alkyl group [24]. This strong *trans* influence of the metal–metal bond has been noted previously [5, 25]. Complexes **1** and **6** represent two limits: (i) the limit in which the Pt–Pt single σ-bond is fully intact, while Z is absent (**1**) and (ii) the limit in which oxidative addition of Z to the Pt(I)–Pt(I) complex has occurred

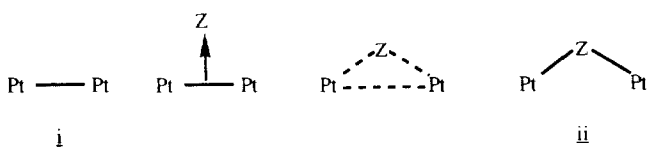

Fig. 2. Schematic representation of two limits: (i) no interaction between Pt(I)–Pt(I) and Z and (ii) Pt(II)–Pt(II) oxidative addition product of the reaction between Pt(I)–Pt(I) and Z, and the intermediate situations.

TABLE 4. $^{31}P\{^1H\}$ NMR spectra of the products **2**, **3**, **4**, **5** and **6** resulting from the reaction of Z with **1**

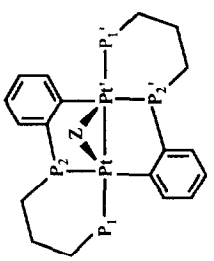

Z (compound)		δP1	δP2	^3J(P1–P1′)	^2J(P1–P2)	^3J(P1–P2′)	^3J(P2–P2′)	^1J(Pt–P1)	^2J(Pt′–P1)	^1J(Pt–P2)	^2J(Pt′–P2)	^2J(Z–P1)
	(1)	+5.6	−26.9	214	21	11	64	1775	996	1860	−143	
$Ag(O_2CCF_3)$	**(2)**	+5.7	−28.0	194	25	n.o.	61	2209	767	1868	−139	46
$Au(PPh_3)^+BF_4^-$[a]	**(5)**	+28.0	−0.2	150	26	0	59	2586	538	1771	−126	
$HgCl_2$	**(3)**	+8.1	−23.6	104	27	−6	54	3066	312	1780	−174	1530
$Hg(O_2CCF_3)_2$	**(4)**	+7.0	−22.6	86	28	−7.2	52	3353	239	1782	−126	2440
I^+I^-[a]	**(6)**	−9.4	−9.8					3719	73	1664	0	

[a]Ref. 11; n.o.: not observed.

to form a Z-bridged Pt(II)–Pt(II) complex in which formally no Pt–Pt single σ-bond is present (**6**) (Fig. 2).

In Table 4 a gradual change in the coupling constants is observed in the series **1, 2, 5, 3, 4, 6**, in which only Z is varied. The values of the coupling constants ^2J(Pt'–P2), ^1J(Pt–P1) and ^2J(Pt'–P1) in **2, 3** and **4** (this work) as well as **5** [11] lie in between those of **1** and **6**. Simulation of the spectra revealed the sign of the various couplings in complexes **2, 3** and **4** (see 'Experimental' and Table 4). The experimental and the simulated spectrum of **4** are shown in Fig. 3. The

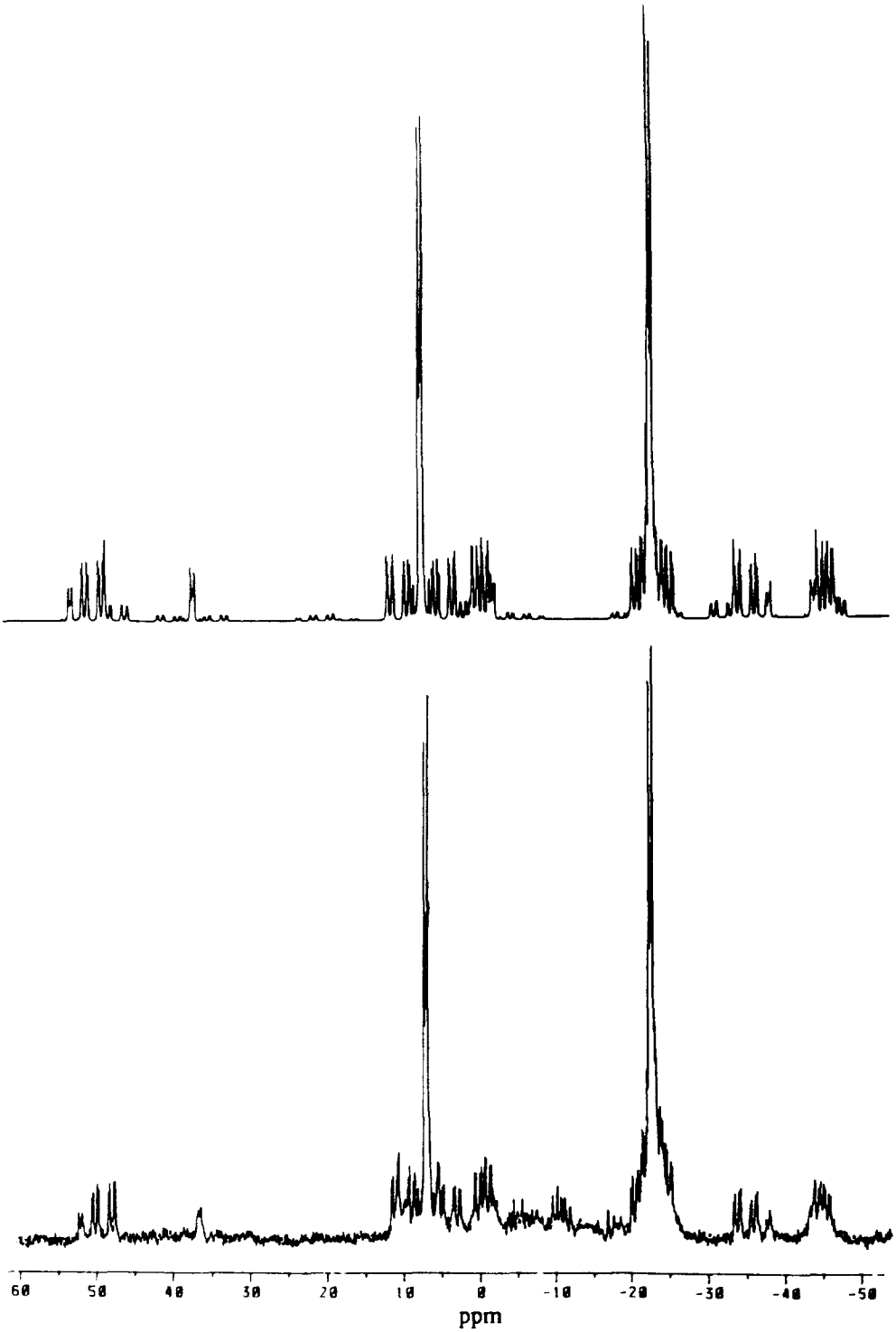

Fig. 3. Experimental and simulated $^{31}P\{^1H\}$ NMR spectrum of compound **4**.

resonances of low intensity were not observed in the experimental spectrum due to a low signal-to-noise ratio and for the same reason the coupling constant ^1J(Pt–Pt') could not be observed.

The presence of these couplings indicates that there is still a Pt–Pt bond present; the decrease in the coupling constants ^1J(Pt'–P2) and ^2J(Pt'–P1) and the increase in ^2J(Pt–P1), all relative to **1**, imply a weakening of the Pt–Pt σ-bond. It has been shown by means of IR spectroscopy that the strength of the Co→Hg(II) bond in $(\eta^5\text{-}C_5H_5)Co(CO)_2 \rightarrow HgX_2$ decreases with decreasing electronegativity of the HgX_2 group in the order $HgCl_2 > HgBr_2 > HgI_2$ [26, 27]. When the interaction between the Pt(I)–Pt(I) dimer and Z is described as a dative $Pt_2 \rightarrow Z$ bond, comparison of the coupling constants ^2J(Pt'–P2), ^2J(Pt'–P1) and ^1J(Pt–P1) of **3** and **4** shows a weaker Pt–Pt bond and a stronger $Pt_2 \rightarrow Hg$ bond in **4** than in the analogous bonds in **3**, owing to the stronger electron-withdrawing properties of the $O_2CCF_3^-$ anion as compared to Cl^-. The stronger $Pt_2 \rightarrow Hg$ bond in **4** relative to **3** is also reflected in the coupling constants ^2J(Hg–P1) of 2440 and 1530 Hz, respectively. These values of ^2J(Hg–P) are in the range of coupling constants found for *trans*-Hg–M–P complexes [28, 29]. In accord with the strength of the $Pt_2 \rightarrow Hg$ bond being dependent on the electronegativity of the metal–complex added, we find a stronger $Pt_2 \rightarrow M$ bond in the order **4** > **3** > **5** > **2**. This can be rationalized by invoking the higher electronegativity of Hg(II) as compared to that of Ag(I) and Au(I). Previously, the bonding of Hg(II) to Ir(I) and Rh(I) has been reported to be stronger than the bonding of Ag(I) to Ir(I) and Rh(I) [28, 30, 31]. The stronger bond of Pt_2 to Au(I) relative to Ag(I) results mainly from the higher electronegativity of the former metal atom [32]. In addition to the platinum–phosphorus coupling constants direct evidence for Pt_2 to Ag(I) bonding was presented by the coupling ^2J(Ag–P1), which amounted to 46 Hz. The same symmetric pattern was observed in the $^{31}P\{^1H\}$ NMR spectrum as was found for **3**, **4** and **5**, which indicates that $Ag(O_2CCF_3)$ is also symmetrically bonded to the Pt–Pt bond.

The X-ray crystal structures of **1** (see footnote on p. 206), **5** [11] and **4** show Pt–Pt distances of 2.656(5), 2.703(1) and 2.7608(7) Å, respectively. These bond lengths are in accord with the decrease in the coupling constants ^2J(Pt'–P2) and ^2J(Pt'–P1) and the increase in ^1J(Pt–P1) when going from **1** via **5** to **4**, which indicate a weakening of the Pt–Pt bond. The weakening of the Pt–Pt bond is the result of a stronger $Pt_2 \rightarrow M$ bond. The results show that the various Pt–P couplings are a good indicator of the strength of the $Pt_2 \rightarrow M$ bond in the adducts of Group 11 and 12 metal atoms to the Pt–Pt bond of $Pt_2\{o\text{-}C_6H_4P(Ph)(CH_2)_3PPh_2\}_2$.

Supplementary material

Full crystallographic details of compound **4** may be obtained from author A.L.S. on request.

Acknowledgements

The Netherlands Foundation for Chemical Research (SON) and the Netherlands Organization for Scientific Research (NWO) are thanked for financial support (A. L. Spek, W. J. J. Smeets). Thanks are also due to A. J. M. Duisenberg for X-ray data collection of $[Pt_2\{o\text{-}C_6H_4P(Ph)(CH_2)_3PPh_2\}_2Hg(O_2CCF_3)_2]$ (**4**). The authors thank K. F. van Malssen (Laboratorium voor Kristallografie, University of Amsterdam) for solving the X-ray structure of $Pt_2\{o\text{-}C_6H_4P(Ph)(CH_2)_3PPh_2\}_2$ (**1**) and D. Heijdenrijk for the collection of those data. We are indebted to Shell Research B. V. for financial support.

References

1 J. Tsuji, *Organic Synthesis by Means of Transition Metal Complexes*, Springer, Heidelberg, 1975, p. 28.
2 F. Glockling, T. McBride and R. J. I. Pollock, *J. Chem. Soc., Chem. Commun.*, (1973) 650.
3 R. Bertani and P. Traldi, *Inorg. Chim. Acta, 134* (1987) 123.
4 P. Lahuerta, R. Martinez-Manez, J. Paya, E. Peris and W. Diaz, *Inorg. Chim. Acta, 173* (1990) 99.
5 D. P. Arnold, M. A. Bennett, M. S. Bilton and G. B. Robertson, *J. Chem. Soc., Chem. Commun.*, (1982) 115.
6 T. J. Barder, S. M. Tetrick, R. A. Walton, F. A. Cotton and G. L. Powell, *J. Am. Chem. Soc., 106* (1984) 1323.
7 A. R. Chakravarty, F. A. Cotton and D. A. Tocher, *Inorg. Chem., 23* (1984) 4697.
8 S. B. Colbran, P. T. Irele, B. F. G. Johnson, F. J. Lahoz, J. Lewis and P. R. Raithby, *J. Chem. Soc., Dalton Trans.*, (1989) 2023.
9 D. P. Arnold, M. A. Bennett, G. M. McLaughlin, G. B. Robertson and M. J. Whittaker, *J. Chem. Soc., Chem. Commun.*, (1983) 32.
10 D. P. Arnold, M. A. Bennett, G. M. McLaughlin and G. B. Robertson, *J. Chem. Soc., Chem. Commun.*, (1983) 34.
11 M. A. Bennett, D. E. Berry and K. A. Beveridge, *Inorg. Chem., 29* (1990) 4148.
12 U. Nagel, *Chem. Ber., 115* (1982) 1998.
13 H. C. Clark and L. E. Manzer, *J. Organomet. Chem., 59* (1973) 411.
14 *CAD-4 User Manual*, Version 5.0, Enraf-Nonius, Delft, Netherlands, 1988.
15 A. L. Spek, *J. Appl. Crystallogr., 21* (1988) 578.
16 N. Walker; D. Stuart, *Acta Crystallogr., Sect. A, 39* (1983) 158.
17 G. M. Sheldrick, *SHELXS86*, program for crystal structure determination, University of Göttingen, FRG, 1986.
18 D. T. Cromer and J. B. Mann, *Acta Crystallogr., Sect. A, 24* (1968) 321.
19 D. T. Cromer and D. Liberman, *J. Chem. Phys., 53* (1970) 1891.

20 G. M. Sheldrick, *SHELX76,* crystal structure analysis package, University of Cambridge, UK, 1976.
21 A. L. Spek, The EUCLID package, in D. Sayre (ed.), *Computational Crystallography,* Clarendon, Oxford, 1982, p. 528.
22 T. Tanase, Y. Kudo, M. Ohno, K. Kobayashi and Y. Yamamoto, *Nature (London), 344* (1990) 526.
23 P. R. Sharp, *Inorg. Chem., 25* (1986) 4185.
24 T. G. Appleton and M. A. Bennett, *Inorg. Chem., 17* (1978) 738.
25 B. R. Steele and K. Vrieze, *Transition Met. Chem., 2* (1977) 169.
26 D. J. Cook, J. L. Dawes and R. D. W. Kemmitt, *J. Chem. Soc. A,* (1967) 1547.
27 D. F. Shriver, *Acc. Chem. Res., 3* (1970) 231.
28 P. I. van Vliet, J. Kuyper and K. Vrieze, *J. Organomet. Chem., 122* (1976) 99.
29 A. Handler, P. Peringer and E. P. Müller; *J. Organomet. Chem., 389* (1990) C23.
30 J. Kuyper, P. I. van Vliet and K. Vrieze, *J. Organomet. Chem., 105* (1977) 379.
31 J. Kuyper and K. Vrieze, *J. Organomet. Chem., 107* (1976) 129.
32 A. S. Kasenally, R. S. Nyholm and M. H. B. Stiddard, *J. Chem. Soc. A,* (1965) 5343.